OPTIMIZATION OF PHOTOELECTRON EMISSION PHYSICAL MODEL IN THE SPACECRAFT INSULATING MATERIAL

Kotaro Suzuki[(1)], Kenji Yabe[(1)], Hiroaki Miyake[(1)], Yasuhiro Tanaka[(1)], Masamichi Ohira[(2)], Teppei Okumura[(2)], Shirou Kawakita[(2)], Masato Takahashi[(2)]

[(1)]Tokyo City University, 1-28-1, Tamazutsumi, Setagaya-ku, Tokyo, 158-8557, Japan , Email:g1681218@tcu.ac.jp
[(2)]Japan Aerospace Exploration Agency, 2-1-1, Sengen, Tsukuba-shi, Ibaraki, 305-8505, Japan

ABSTRACT

Since photoelectron emission (P.E.) is dominant in the charging of satellites which are operated under insolation conditions, the P.E. current is one of most important parameter for the determination of surface electric potential. Therefore, we have focused on P.E. and are developing research for it. We have also evaluated P.E. using quantum efficiency which is calibrated by the illuminate light quantity. Since the current empirical formula is deduced from limited measurement materials, it is better that we provided a new formula of P.E. related to physical phenomenon. We focused on the P.E. model formula given by W.E.Spicer. From this model formula, we considered the relationship between coefficients and the value of physical properties. As a result, we succeed in obtaining the optimized formula for polymeric material compared with the experimental value. In this report, we introduced the model with detailed explanation and the comparison between the model and experiment results.

1. INTRODUCTION

In recent years, a number of spacecraft, such as satellites and spacecraft are operated in space. However, abnormal operation due to charging and discharging is occurring at present [1]. In order to achieve high reliability and a long life of spacecraft surface materials, it is important to study the charging and discharging properties of the insulating materials being used. To suppress the charging and discharging of spacecraft surface materials, it is necessary to understand the charging characteristics of insulating materials, and evaluate the amount of charge in the orbit from the design stage. The main factors behind the charge of satellites in orbit, are electrons, protons, and, solar energy. Especially photoelectron emission caused by sunlight becomes dominant among charges under sunlit conditions. Consequently, quantum efficiency which can quantitatively evaluate photoelectron emission, is an important physical properties value. Therefore, our research group constructed a photoelectron emission current measuring device to calculate the quantum efficiency. We evaluated the ionizatiom energy of the materials from the quantum efficiency and the photoelectron emission characteristic curve of spacecraft surface materials, since numerical calculation

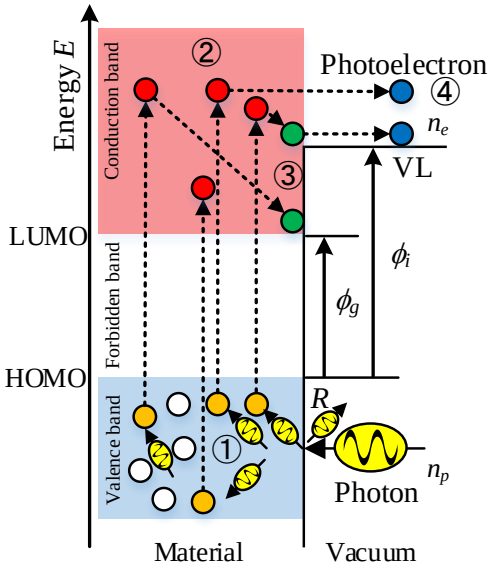

Figure 1. Emission process of photoelectron emission

is used to evaluate charge in the design state, a formula of physical properties of photoelectron emission conforming to the actual measurement value is required. Furthermore, to extend the life of a satellite, considering only by measuring the physical properties value will not be enough. There would be a need to understand the charging phenomena by constructing a physical model of how energy electrons in the material receive and release the irradiation photon. In this paper, we report below the photoelectron releasing physical model which we constructed from the photoelectron generation and releasing process.

2. PHOTOELECTRON EMISSION PROCESS

Fig. 1 shows the photoelectron emission model when light is irradiated. We thought that the light emission in reference to the model of Spicer [2] has the following four processes.

①Absorption process of light within the bulk of the material

②Electron excitation process by light absorption

③Surface reaching process of excited photoelectron

④Surface escape process of photoelectrons that have reached the surface

We compared each process with Fig. 1. ①Absorption process of light is $A(h\nu)$, ②Electron excitation process is $c_e(h\nu)$, ③ Surface reaching process of excited photoelectron is $P_L(h\nu)$, ④Surface escape process of photoelectrons is $P_S(h\nu)$. As written above, by integrating the four parameters, the quantum efficiency $\eta(h\nu)$ can be expressed as Eq. (1).

$$\eta(h\nu) = A(h\nu) \times C_e(h\nu) \times P_L(h\nu) \times P_S(h\nu) \quad (1)$$

Absorption process of light is an amount photons emitted in the material is absorbed into the material. This is shown in the first term of the right-hand side of Eq. (1). Electronic excitation process due to absorption of light is the number of photoelectrons excited to or higher than VL per photon. This is shown in the second term of the right-hand side of Eq. (1). Surface arrival process of excited photoelectron, is the attenuation ratio of when the photoelectrons excited to or higher than VL reaches the material surface. This is shown in the third term of the right-hand side of Eq. (1). Surface escape process of photoelectrons which has reached the surface, is the probability of electrons emitted from the surface of the material into vacuum. This is shown in the fourth term of the right-hand side of Eq. (1). A detailed description of each process are shown below.

2.1. Absorption process of light within the bulk material

When light enters a material, the light inside the length of the material z will natural logarithmic be absorbed by the rate of absorption coefficient $\alpha(h\nu)$. When a number of photons n_p is irradiated to the material, the relationship between the reflectivity of light R, absorption $A(h\nu)$, and the transmittance $T(h\nu)$ can be expressed by Eq. (2).

$$A(h\nu) = n_p(1-R)(1-e^{-\alpha(h\nu)z}) \quad (2)$$

Absorption of light in the material is assumed to occur until the thickness of the material L ($z = L$). Also $\alpha(h\nu)$ is calculated from Tauc Plot type of Eq. (3) [3].

$$\alpha(h\nu) = \frac{B(h\nu - \phi_g)^n}{h\nu} \quad (3)$$

B: Proportionality constant of each material
ϕ_g: Energy gap [eV]
n: 1/2 or 2 (Differs depending on the structure of the energy bands. 1/2 for direct transition and 2 for the indirect transition)

2.2. Electron excitation process by light absorption

Fig. 2 shows the conduction electron distribution of the insulator. Figure 2 shows: (a) the electron density of states $D(E)$, (b) the electron occupation probability $f(E)$, (c) the electrons distribution $n(E)$. From Fig.2, the electron distribution $n(E)$ can be calculated by

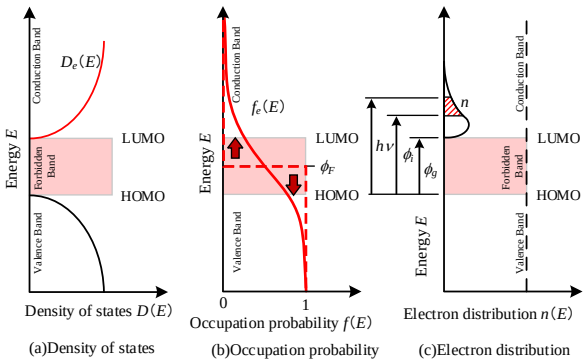

Figure 2. Conduction electron distribution of the insulator

$$C_e(h\nu) = \int_{\phi_i}^{h\nu} n(E)dE = \int_{\phi_i}^{h\nu} D(E)f(E)dE \quad (4)$$

multiplying the electron density of states D (E) and the electron occupation probability f (E) together then, integral to $h\nu$, which is expressed by Eq. (4).
At this point, E is the electron energy [eV]. We considered the excitation of or a higher level than VL in the devised model. Thus, Eq. (4) of the integration interval is from the ionization energy ϕ_i to the irradiation photon energy $h\nu$. (However, in the case of $\phi_g > \phi_i$ the integration interval would be from ϕ_g to $h\nu$) In this case, we use the measurement limit value of the experiment for ϕ_i (ϕ_g). The electron density of state D (E) and the electron occupancy probability f (E) can be calculated by Eq. (5), (6).

$$D(E) = 4\pi\left(\frac{2m_e}{h^2}\right)^{\frac{3}{2}}\sqrt{E-\phi_g} \quad (5)$$

$$f(E) = e^{-\frac{(E-\phi_F)}{kT}} \quad (6)$$

m_e is the electron effective mass [kg], ϕ_F is the Fermi level energy [eV](In the case of insulating materials $\phi_F = \phi_g/2$), k is the Boltzmann's constant [eV/K], T is the temperature of material [K]. The electron density of states D (E) is a numerical value of unit volume and state per unit energy. This represents the density of energy levels that electrons can be enter. The electron occupation probability f (E) is the probability density function that electrons actually occupy in the level of energy E. When we calculate m_e, it represents the mass of electron. f (E) which is understood to be dependent on the material temperature T. Thus this time, f (E) was calculated assuming that all of the irradiation light energy $h\nu$ is converted to excitation energy.

2.3. Surface reaching process of excited photoelectron

Fig. 3 shows the relationship between the position the photoelectrons are generated and the surface reaching

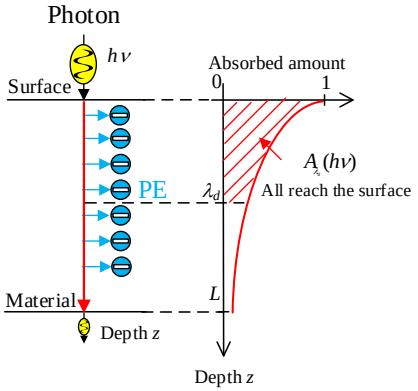

Figure 3. Relationship of the generated photoelectrons position and surface arrival probability

probability of excited electrons of the proposed model. When we propose the surface reaching probability P_L ($h\nu$), we assume that all of the photoelectron on the surface side than the average escape depth λ_d of electrons, reach to outermost surface, photoelectrons within the bulk side cannot. In addition, when photoelectron generation rate due to photon is assumed to be constant without depending on the material depth, surface reaching probability P_L ($h\nu$) is considered to be as Fig. 5 (right) and can be calculated by Eq. (7).

$$P_L(h\nu) = \frac{A_{\lambda d}(h\nu)}{A(h\nu)} \tag{7}$$

$A_{\lambda d}$ ($h\nu$) is the amount of light absorbed up to the average escape depth λ_d ($z = \lambda_d$). Average escape depth λ_d is calculated by the experience type of mean escape depth λ_d [nm] and electronic energy E [eV] that M. P.Seah proposed [4].

$$\lambda_d = \frac{\lambda_0}{\rho} = \frac{49E^{-2} + 0.11E^{1/2}}{\rho} \tag{8}$$

In the process of photoelectrons being excited to the surface, the energy E_p(= $h\nu$-ϕ_i) needed for the photoelectrons to be excited is, from the ionization energy of the material, about 10 eV at maximum. When calculating Eq. (8), E is set to constant. We used the average value from the minimum energy possible to be measured by M.P.Seah (E_p = 1 ~ 10 eV) up to the energy we required for E.

2.4. Surface escape process of photoelectrons reach the surface

This time, the photoelectron of surface escape probability P_S ($h\nu$) is the function of the irradiation photon energy $h\nu$. We considered that when irradiation photon energy $h\nu$ becomes higher, the surface escape probability P_S ($h\nu$) can be expressed as an increasing exponential function. This was expressed in Eq. (9). F_1, F_2 that is shown in Eq. (9) cannot be determined by calculation. It was calculated from the regression coefficients of the measured values.

$$P_S(h\nu) = F_1 e^{(E_P \times F_2)} \tag{9}$$

2.5. Model that takes into account the photoelectron emission process

Eq. (1) - (9) shows a model considering photoemission process in Eq. (10). We optimize upon some materials on Eq. (10). After we calculated the regression coefficient F_1, F_2 of each material, we found a correlation between the material physical properties. In this way, the photoelectron emission physical model can be constructed.

$$\eta(h\nu) = (1-R)\left(1 - e^{-\frac{B(h\nu-\phi_g)^n}{h\nu}\frac{7.84}{\rho}}\right) \times \int_{\phi_i}^{h\nu} D(E) f(E) dE \times F_1 e^{(E_P \times F_2)} \tag{10}$$

3. OPTIMIZATION FOR THE MEASURED VALUE

We show the calculation conditions and the calculation result of when doing the regression calculation using Eq. (10).

3.1. Calculation conditions

Regression calculation conditions are as below.

①Assume that the number of photon n_p = 1 /m^{3}s is eradiated to the material.

②When photon is eradiated to material R = 0.

③The measuring limit value of measurement is used for ϕ_i.

④m_e is electron mass.

⑤ All the photon energy that is absorbed into the material is converted to excitation energy.

3.2. Calculation results

Comparison of quantum efficiency of calculated value and measurement value upon fluorine-based materials ETFE, PVDF, FEP), polyimide-based materials(PI_1, PI_2) derived from Eq. (10)are shown in Fig.4. Vertical axis is quantum efficiency $\eta(h\nu)$, horizontal axis is wavelength λ and energy conversion value $h\nu$ are shown. Plots shown in the figure are the measurement value. Calculation value by Eq. (10) is shown in a solid line. A large difference can be confirmed in the wavelength nearby ϕ_i although from same figure, the calculation value and the measurement value have the

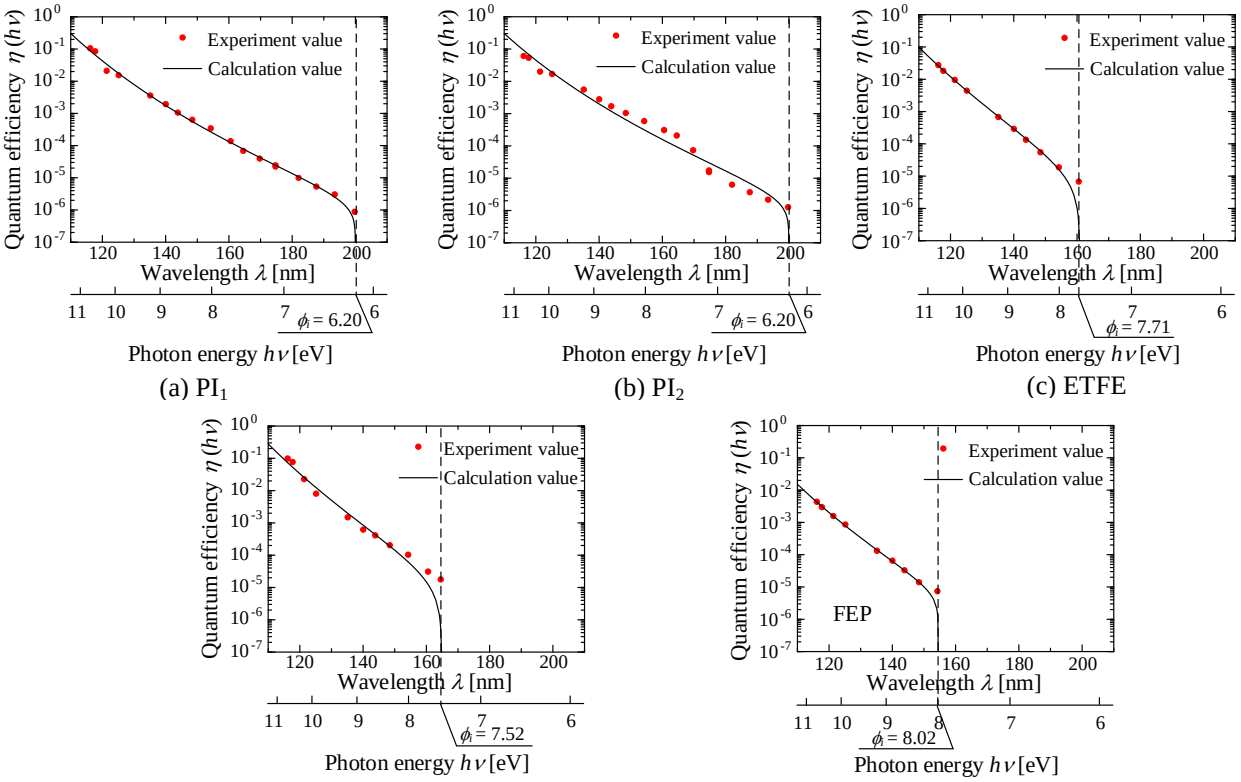

(a) PI_1 (b) PI_2 (c) ETFE

(d) PVDF (e) FEP

Figure 4. Optimization in the experimental value

same tendency and digit. This is because the measuring limit value is set to ϕ_i. Photoelectron emission is the phenomena when $h\nu \geqq \phi_i$ photon electron emission occurs, when $h\nu < \phi_i$ photo emission doesn't occur. Therefore, the calculation results of when the quantum efficiency settles to 0 shows the photoelectron emission characteristics.

4. THE CONSTRUCTION OF THE PHOTOELECTRON EMISSION PHYSICAL MODEL

4.1. The function of regression coefficient and material property value

Tab. 1 shows the achieved regression coefficient F_1, F_2 for each material by the regression calculation used in Eq. (10).

Table 1. Regression coefficient of each material

Define	F_1	F_2
PI_1	1.06E-05	1.76
PI_2	1.94E-05	1.69
ETFE	7.82E-03	1.83
PVDF	1.58E-02	1.87
FEP	3.92E-03	1.83

As written in the previous chapter, F_1, F_2 can be predicted by comparing and considering the regression coefficient F_1, F_2 as the function of the material properties value, obtained by the regression calculation against the measurement value. The characteristics of the photoelectron emission can be calculated by using the irradiation photon energy $h\nu$ and the material properties value, since F_1, F_2 that could not be evaluated with the regression calculation, can be evaluated by substituting material properties value.

Surface escape phenomena is a phenomenon in which the material is ionized. It is considered that there is electron affinity χ and correlation that occurs when ionized. We physically considered the phenomena of the electrons escape which has reached the surface. It is considered that there is a correlation with the material density ρ. We drew a graph of the relationship between the electron affinity χ and the regression coefficient F_1, between material density ρ and regression coefficient F_2. Electron affinity χ and regression coefficient F_1 are related. Material density ρ and the regression coefficient F_2 are also related. The relationship of the regression coefficient F_1 and χ in each of the material is shown in Fig. 5. Vertical axis shows the regression coefficient F_1, and the horizontal axis the electron affinity χ [eV]. The solid line in the figure is the approximate line with

respect to F_1, it shows the approximate expression in Eq. (11). From the considered Eq. (11) and Fig.5, when the electron affinity χ increases, F_1 reduces. Consequently, photoelectron emission is less likely to occur. Electron affinity is the energy that occurs when it becomes anion.

The parameter shows how easy it is to anion. In construct, electron emission is the phenomena of becoming a cation. Therefore it is believed that the attenuation tendency of F_1 was confirmed with the increasing electron affinity.

Fig. 6 shows the relationship between the regression coefficient F_2 and the material density ρ in each material. Vertical axis indicates the regression coefficient F_2, horizontal axis the material density ρ [g/cm^3]. The solid line is an approximate straight line for F_2 in Fig.6. Eq. (12) shows its approximate expression. Eq. (12) and Fig. 6 show that when the material density ρ becomes larger, F_2 also increases. In other words, photoelectron emission becomes easier. The reason for this can be considered as following. If the material density increases, the mean free path of the photoelectrons migrating to the surface when you try to return to the direction of the bulk decreases. Therefore, since it cannot deeply advance to the direction of the bulk, the photoelectron emission amount increases, it is believed that the increasing of F_2 with increase of the material density.

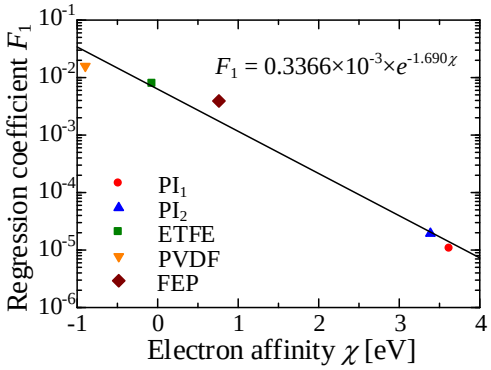

Figure 5. Relationship between F_1 and χ of each material

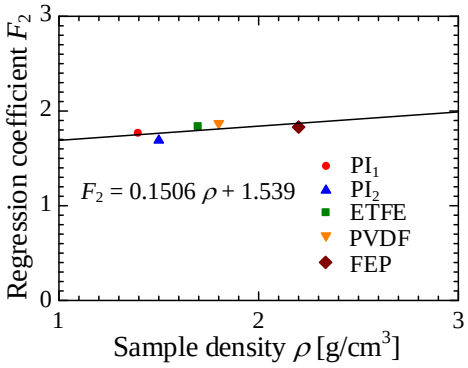

Figure 6. Relationship between F_2 and ρ of each material

$$F_1 = 0.3366\times10^{-3}\times e^{-1.690\chi} \quad (11)$$

$$F_2 = 0.1506\rho + 1.539 \quad (12)$$

4.2. Photoelectron emission physical model

The comparison of quantum efficiency of the calculated value and the measurement value and the optimization upon fluorine-based materials ETFE, PVDF, FEP), polyimide-based materials (PI_1, PI_2) derived from Eq. (10) – (12) are shown in Fig.7. The calculation value and the measured value have the same tendency and digit in Fig.7. Furthermore, it also shows the characteristics of photoelectron emission because quantum efficiency settles to 0 in ϕ_i.

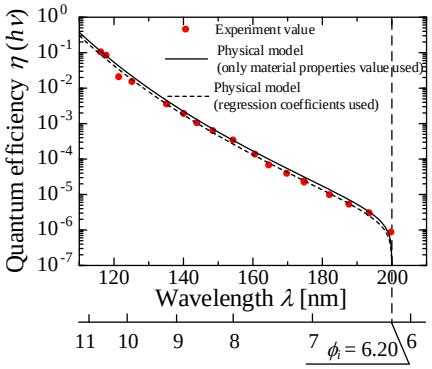

(a) PI_1

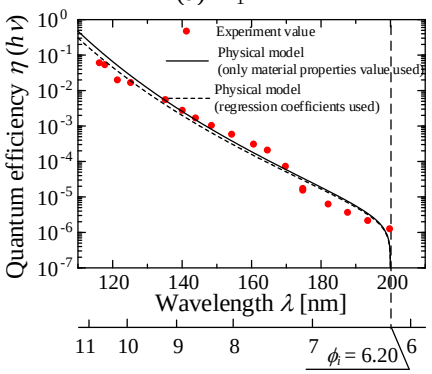

(b) PI_2

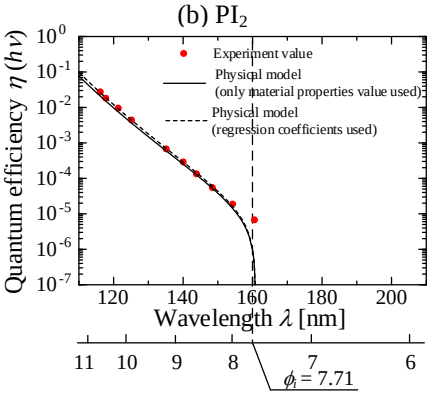

(c) ETFE

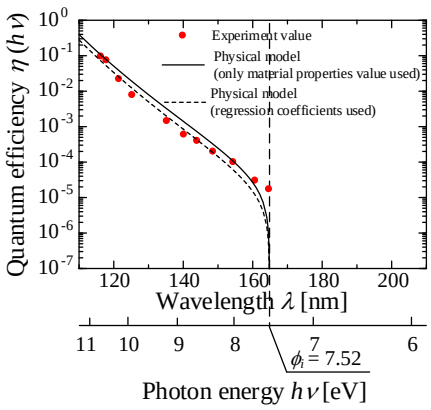

(d) PVDF

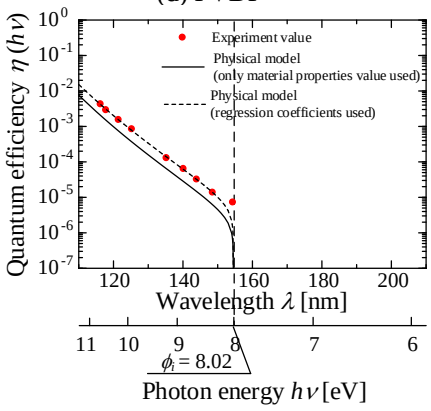

(e) FEP

Figure 7. Comparison between the experimental value and the photoelectron emission physical model

5. SPECIFIC MATERIAL PROPERTIES VALUES THAT BRING AN INFLUENCE ON PHOTOELECTRON EMISSION BY SENSITIVITY ANALYSIS

5.1. How to identify

Photoelectron emission physical model constructed in the previous section is not only fit for the measured value, but it can be calculated only by the material properties value. Furthermore, it is a model in consideration of a physical phenomenon (photoelectron emission process). Therefore, performing a sensitivity analysis for each material properties value, it may also be possible to identify the material properties value that has the largest influence on photoelectron emission.

When performing a sensitivity analysis, the result of the photoelectron emission physical model will be the standard. From there we can evaluate by the mean absolute error. We show the example of the calculation in Fig. 8. Fig. 8 shows the photoelectron emission physical model result in PI_1. It shows comparison of the calculation results of when ionization energy is 15 %,-15% with the material density of 15 %,-15%. Fig. 8 shows that the result of when varying ionization energy, deviate significantly from the results of the photoelectron emission physical model. However, the fluctuation of the result of varying material density is smaller than the result of varying ionization energy. As suggested above, it can be seen that ionization energy has more effect on photoelectron than material density in PI_1. From the above reasons, reflectance R, ionization energy ϕ_i, energy gap ϕ_g, average escape depth λ_d, and density ρ of each material are shown below.

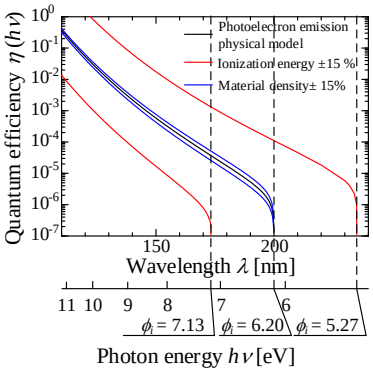

Figure 8. Example of calculation of the mean absolute error (PI_1)

5.2. Specific material property value that bring an influence on photoelectron emission

Tab. 2, 3 shows the material properties value of when performing the sensitivity analysis of PI_1, ETFE. Each table for each variation rate -30%, -15%, 15%, 30% shows the material properties value. In other words, the value at 0% is the value that is substituted for the photoelectron emission physical model.

Tab. 4, 5 shows the sensitivity analysis results of PI_1, ETFE (the result of average absolute error from the photoelectron emission physical model). Color coding of each table is indicated by percentile and color bar. Value at 0 shows that the model has not changed in Tab.4, 5.

Both results show the following. Ionization energy affects the photoelectron emission the most. It can be confirmed that the energy gap of the physical properties value effects the second. Ionization energy and energy gap related to energy band structure from each result is influential with respect to photoelectron emission phenomenon. Density and average escape depth was found to be independent. Thus, it can be seen that the measurement of ionization energy and energy band becomes important in order to discuss photoelectron emission.

Table 2. Material physical properties for use in the analysis (PI_1)

Parameter variation rate	-30%	-15%	0%	15%	30%
Reflectance R	-	-	0	0.15	0.3
Ionization energy ϕ_i	4.34	5.27	6.2	7.13	8.06
Energy gap ϕ_g	1.801955	2.1880882	2.5742214	2.9603546	3.3464879
The average escape depth λ_d	3.921E-09	4.761E-09	5.601E-09	6.441E-09	7.281E-09
Density ρ	0.98	1.19	1.4	1.61	1.82

Table 3. Material physical properties for use in the analysis (ETFE)

Parameter variation rate	-30%	-15%	0%	15%	30%
Reflectance R	0	0	0	0.15	0.3
Ionization energy ϕ_i	5.39801	6.5547264	7.7114428	8.8681592	10.024876
Energy gap ϕ_g	5.4435715	6.6100512	7.7765308	8.9430104	10.10949
The average escape depth λ_d	3.229E-09	3.921E-09	4.612E-09	5.304E-09	5.996E-09
Density ρ	1.19	1.445	1.7	1.955	2.21

Table 4. The sensitivity analysis results (PI_1)

Parameter variation rate	-30%	-15%	0%	15%	30%
Reflectance R	-	-	0	0.010	0.008
Ionization energy ϕ_i	9.481	2.633	0	2.090	8.616
Energy gap ϕ_g	0.131	0.007	0	0.102	0.302
The average escape depth λ_d	0.010	0.009	0	0.012	0.026
Density ρ	0.093	0.059	0	0.010	0.020

Table 5. The sensitivity analysis results (ETFE)

Parameter variation rate	-30%	-15%	0%	15%	30%
Reflectance R	0	0	0	0.015	0.047
Ionization energy ϕ_i	16.709	4.343	0	5.248	21.754
Energy gap ϕ_g	3.384	0.912	0	0.649	2.860
The average escape depthλ_d	0.047	0.015	0	0.005	0.004
Density ρ	0.109	0.012	0	0.073	0.231

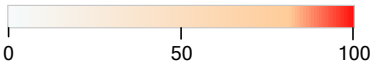

6. CONCLUSION

In this paper, based on the emission process of photoelectrons applied in the Spicer model, the measured value of the insulation material for the spacecraft coincided. A physical model which can obtain photoelectron emission characteristics by using only material property values was constructed in order to perform clarification of photoelectron emission phenomena. The physical model is thought to be able to obtain the photoelectron characteristics, since the constructed physical model is in line with the actual measured value in all of the materials. We did a sensitivity analysis. The photoelectron emission phenomena has the largest influence caused by the ionization energy and the energy gap which relates with the energy band structure. However, density and average escape depth was found to be independent. Thus, it can be seen that measuring the ionization energy and the energy band are important in order to discuss photoelectron emission.

7. REFERENCES

1. H. C. Koons, J. E. Mazur, R. S. Selesnick, J. B. Blake, J. F. Fennell, J. L. Roeder, and P. C. Anderson. (1998). The impact of the space environment on space systems, Proc. of the 6th Spacecraft Charging Technology Conference, Air Force Research Laboratory, AFRL-VS-TR-20001578, pp. 7-11.
2. W. E. Spicer. (1958). Photoemissive, Photoconductive, and Optical Absorption Studies of Alkali-Antimony Compounds, Phys. Rev. 112, Issue.1, pp.114-122.
3. J. Tauc et al. (1966). Optical Properties and Electronic Structure of Amorphous Germanium, Phys. Stat. Sol. 15, Issue.2,pp.627-637.
4. M.P.Seah et al. (1979). Surf. Interface Anal. 1, No.1.